metals

MDPI

Article

Effect of Al5TiB Master Alloy with P on Microstructure and Mechanical Properties of AlSi7Mg Alloy

Tomasz Lipiński

Faculty of Technical Sciences, University of Warmia and Mazury in Olsztyn, 10-719 Olsztyn, Poland; tomaszlipinski.tl@gmail.com

Abstract: Aluminum-silicon alloys are popular casting alloys. In its raw state, the microstructure of the hypoeutectic silumin consists of a large eutectic β phase against the background of dendritic eutectic α. Due to its large microstructure components, mainly the eutectic β phase, this alloy has low mechanical properties. The unfavorable properties of hypoeutectic silumin can be improved by changing the size and shape of the alloy's microstructure components. There are several possibilities for controlling the microstructure and the resulting mechanical properties of the alloy. One possibility is to modify the alloy with elements and chemical compounds. This paper presents the effect of phosphorus with Al-Ti-B on the microstructure and mechanical properties of hypoeutectic silumin AlSi7Mg. The proportions of Ti to B were selected on the basis of the results presented in the literature, recognizing the optimal ratio of 5:1. The modifier was introduced into the alloy in the form of an AlTiBP master alloy with a variable content of titanium, boron, and phosphorus. Phosphorus was added at the levels of 0.1, 0.2, and 0.3% of the weight of the modified casting. As a result of the tests carried out, the modifying effect of the introduced master alloy was confirmed. A different morphology of microstructures was obtained for the different chemical compositions of the modifier. The most favorable modification effect, whose measurable parameter is the highest (out of the obtained) mechanical properties, was found for the modifier containing 0.25% Ti + 0.03% B + 0.2% P. It was also found that phosphorus, in the presence of titanium and boron, affects the microstructure and mechanical properties of hypoeutectic silumin AlSi7Mg.

Keywords: Al-Si alloys; hypoeutectic silumin; modification; modifier

Citation: Lipiński, T. Effect of Al5TiB Master Alloy with P on Microstructure and Mechanical Properties of AlSi7Mg Alloy. *Metals* **2023**, *13*, 1560. https://doi.org/10.3390/met13091560

Academic Editors: Ricardo Branco and Filippo Berto

Received: 18 August 2023
Revised: 29 August 2023
Accepted: 4 September 2023
Published: 6 September 2023

1. Introduction

Cast metal alloys are a popular group of construction materials. Among them are light metal alloys, which include, among others, aluminum alloys. Cast aluminum-silicon alloys are characterized, among others, by a relatively low casting temperature, good castability, ease of filling the mold, low specific gravity, and relatively high mechanical and corrosion properties [1–7]. In hypoeutectic Al-Si alloys, the α phase is the first to crystallize. Its heat from crystallization heats the remaining liquid to a liquidus temperature. The crystallization front of the α-phase dendrites ejects the silicon atoms into the liquid. It is enriched in Si with continuous lowering of the temperature. The process of crystallization of the α phase dendrites lasts up to the solidus temperature. At this temperature, due to the supersaturation of the remaining liquid with silicon, the crystallization of the α+β eutectic begins, in which silicon is the leading phase. The β phase is a good catalyst for the nucleation of the α phase, and, in the process of eutectic crystallization, the α solid solution nucleates and grows [8–13]. The primary hypoeutectic aluminum-silicon alloy crystallizes to form a dendritic α-phase microstructure and a coarse-grained α+β eutectic. The presence of acute-angled crystals of the β phase (almost pure Si) in silumins is the reason for the unfavorable performance properties of the alloy. This is the reason for many years of work aimed at refining the microstructure and thus increasing the mechanical

properties of the alloy [14,15]. The microstructure, and therefore the properties of silumins, can be shaped, among others, by:

- Modification [16–18], including, among others, with: calcium [19], sodium [20], sodium chloride [21,22], exothermic mixtures based on natrium [23,24], mischmetal [25], strontium [26,27], lithium [28], scandium and yttrium [29,30], antimony [31], titanium [32–34], boron [35], and modification with a homogeneous modifier with a composition similar to a worked alloy (or made from a worked alloy) [36];
- Introduction of alloy additions [37–39];
- Directional crystallization process [40–43];
- Manufacturing process [44–48];
- Heat treatment [49,50].

In practice, several methods are used simultaneously to influence the structure [51–55]. Phosphates (e.g., $NaPO_3$) [56] and Na halides (e.g., NaF and NaCl) [1,21,57] have also been successfully used as mixtures. The influence of phosphorus on the modifications of primary silicon in hypereutectic and eutectic silumins is described in the literature [58]. According to the theory, eutectic silumins do not have a primary β phase, and their microstructure (taking into account the coupled zone) is a eutectic composed of α+β. This eutectic occurs in hypoeutectic silumins against the background of the α phase. If the research results known from the literature show the influence of the phosphorus introduced in the master alloy on the properties of the eutectic silumin, then there may be an analogous effect of the master alloy containing phosphorus on the eutectic of the hypoeutectic silumin, whose properties depend on the properties of the hypoeutectic Al-Si alloy.

Numerous studies also show the possibility of refining the microstructure of hypoeutectic silumin and increasing its mechanical properties using the Al-Ti-B master alloy [59,60] or in combination with strontium [61–63] or other elements [64,65]. Studies conducted on the Al10%Si035%Mg alloy with the addition of Al1.5%Ti1.5%B and Sr showed a low effect of Sr modification and a good refining effect by the action of the Al-Ti-B master alloy [66,67]. The effect of eliminating the impact of any of the tested ingredients as improvers (modifiers and refiners) was not observed. It can therefore be assumed that the interaction of both modifying components depends on their percentage content in the alloy. The effect can be explained by the master alloy composition (Al1.5%Ti1.5%B + Sr), which is similar to the stoichiometric composition of the SrB_6 phase. The presence of TiB2 particles in the grains of the β phase was observed in this study, which confirms the assumption about the influence of this compound on the crystallization process. The formation of free AlB_2 and Sr particles contributes to the formation of the SrB_6 phase. The formation of this phase is accompanied by the local capture of both Sr and B, which play a very important role in the formation of the phase morphology of the Al-Si alloy. After Al-Ti-C-Sr modification, as exemplified with the Al7Si alloy, the presence of TiC and Al4Sr phases in the α phase matrix, which is attributed to the α phase [68] modifying effect, was observed, similarly to the Al_3Ti phase [69]. The use of only boron to modify Al10Si silumin did not have the expected effect. The eutectic β phase was fragmented to a small extent [70]. However, the use of B in combination with Al, Ca, and Si (AlxCamBnSi) caused the modification of the primary β phase [35]. The refining effect of Al7Si silumin was confirmed for the Al-Ti-B master alloy [71,72]. The effect is the greater when more boron is introduced [71]. The AlTi5B1 alloy in the form of a wire can be used for grain refinement in cast Al alloys. In a number of papers, the optimal ratio of Ti:B was set at 5:1, and the refining effect of the AlTi5B1 alloy was attributed to the TiB_2 and Al_3Ti phases [72–76].

Using the ratios of Ti:B as 5:1 given by other researchers and taking into account the results of research confirming the modifying effect of phosphorus on the morphology of primary silicon (although present in hypereutectic silumins) and phosphates on modifications of the α+β eutectic, it was decided to check the effect of phosphorus in the presence of Al-Ti-B on the microstructure and mechanical properties of hypoeutectic silumin.

2. Materials and Methods

The tests were carried out on a hypoeutectic AlSi7Mg alloy, with the real chemical composition shown in Table 1 [54].

Table 1. Contents of chemical composition tested hypoeutectic basic AlSi7Mg alloy.

Chemical Element	Si wt. %	Mg wt. %	Mn wt. %	Fe wt. %	Cu wt. %	Ni wt. %	Ti wt. %	B wt. %	Al wt. %
Average contents	7.24	0.30	0.26	0.13	0.10	0.006	0.00	0.00	bal.

This alloy was obtained from industrially produced ingots. In order to standardize the chemical composition of silumin, it was subjected to initial melting at 800 °C for 30 min in a ceramic crucible with a capacity of 5 L. The melted alloy was cast into steel fittings. Melts of Al-Ti-B-P master alloys were carried out in a ceramic crucible with Al_2O_3 placed in an electric furnace chamber. The composition of master alloys was matched to the weight of the modified silumin, taking as a criterion the content of chemical elements introduced into the silumin. The contents of titanium, boron, and phosphorus in terms of the weight of the casting (introduced into silumin) are listed in Table 2.

Table 2. Content of components in the modifier for the mass of the casting.

Plan Point	Chemical Element			
	Ti wt. %	B wt. %	P wt. %	Al wt. %
non	0	0	0	0
AlTi0.05B0.01P0.1	0.05	0.01	0.1	Bal.
AlTi0.15B0.03P0.1	0.15	0.03	0.1	Bal.
AlTi0.25B0.05P0.1	0.25	0.05	0.1	Bal.
AlTi0.35B0.07P0.1	0.35	0.07	0.1	Bal.
AlTi0.45B0.09P0.1	0.45	0.09	0.1	Bal.
AlTi0.05B0.01P0.2	0.05	0.01	0.2	Bal.
AlTi0.15B0.03P0.2	0.15	0.03	0.2	Bal.
AlTi0.25B0.05P0.2	0.25	0.05	0.2	Bal.
AlTi0.35B0.07P0.2	0.35	0.07	0.2	Bal.
AlTi0.45B0.09P0.2	0.45	0.09	0.2	Bal.
AlTi0.05B0.01P0.3	0.05	0.01	0.3	Bal.
AlTi0.15B0.03P0.3	0.15	0.03	0.3	Bal.
AlTi0.25B0.05P0.3	0.25	0.05	0.3	Bal.
AlTi0.35B0.07P0.3	0.35	0.07	0.3	Bal.
AlTi0.45B0.09P0.3	0.45	0.09	0.3	Bal.

The weight of aluminum was selected in such a way that titanium, boron, and phosphorus accounted for about 10% by weight in the master alloy. The diagram of the casting mold used for all heats is shown in Figure 1 [54].

For the production of master alloys, titanium in the form of powder with a purity >98.5%, boron in the form of boron puriss p.a. crystalline pieces with a purity of >95%, phosphorus in the form of powder with a purity of >98%, and aluminum in the form of ingots with a purity of >98% were used. The molten master alloy was cast into a cylindrical metal mold with a diameter of 8 mm and then mechanically ground to a grain fraction of 0.8–1.2 mm. The modification was carried out on about 750 g of silumin for each of the

heats. A new AlSi7Mg alloy was used for each melt. The modification was carried out in a crucible at a temperature of 780 °C for 20 min, after which the alloy was poured into a casting mold.

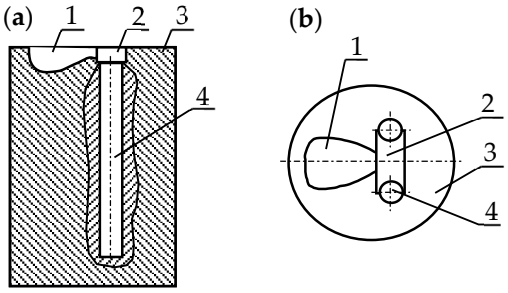

Figure 1. The diagram of the casting mold: 1—pouring cup, 2—sprue, 3—mold, 4—casting (samples): (**a**) section, (**b**) top view.

Metallographic examinations were carried out using an Olympus IX70 optical microscope. Mi8Al reagent was used for etching metallographic samples. Phase analysis was performed using an X-ray phaser Bruker diffractometer with Difrac EVA and HighScore Plus software and the ICDD PDF-4 + crystallographic database. The static tensile test was carried out on a ZD10 machine on five-fold cylindrical samples with a measuring diameter of 6 mm according to EN ISO 6892-1:2016 [77]. Two samples for each heat were tested. Brinell hardness was tested on the heads of samples prepared for a static tensile test in accordance with ISO 6506-1:2014 [78] using a ball with a diameter of 2.5 mm, a load of 306.5 N, and a load time of 20 s in the HPO 250 hardness tester. Three measurements were made on each sample. The arithmetic mean of the measurements was used for the analysis.

3. Results and Discussion

The microstructure of the AlSi7Mg alloy cast into the mold without modification is shown in Figure 2a. It consists of thick, uneven plates of the eutectic β phase against the background of the α phase. The occurrence of a disordered distribution of the β-phase plates and their unregulated thicknesses prove the lack of thermodynamic stabilization in the crystallization process. This microstructure is reflected in low mechanical properties. Tensile strength Rm = 136 MPa (Figure 3a), elongation A = 0.7% (Figure 3b), and Brinell hardness H = 51 HB (Figure 3c). After introducing a master alloy based on aluminum AlTi0.05B0.01P0.1 containing 0.05% titanium + 0.01% boron + 0.1% phosphorus in relation to the mass of modified silumin, the process of stabilization of the α+β eutectic crystallization was found (Figure 2b). A clear reduction in the grain size of the β phase (a solid solution of aluminum in silicon) was observed. The remaining thick, unmodified β phase had an elongated form resembling thick, short plates. The formation of the eutectic was clearly visible, enabling visual separation of the eutectic from the primary α phase (solid solution of silicon in aluminum), which had begun to assume the dendritic form. The effect of fragmentation and partial, basically initial, ordering of the α+β eutectic was an increase in mechanical properties to Rm = 153 Mpa, A = 2.5%, and H = 56 HB (Figure 3). After modification of the silumin with AlTi0.15B0.03P0.1 containing 0.15% titanium + 0.03% boron + 0.1% phosphorus, a further increase in the order of the microstructure was found (Figure 2c). A definite further reduction in the size of the β phase to a plate-like size and shape was found. There was already a clear separation of the α+β eutectic and the primary dendritic α phases. It was possible to already observe the axes of the main silicon wafers parallel to each other. This fact is a testament to the beginnings of thermodynamic stabilization of the crystallization of the α+β eutectic. The effect of the beginnings of modification of the microstructure was an increase in the mechanical properties of the AlSi7Mg alloy to Rm = 171 Mpa, A = 4.5% and H = 61 HB (Figure 3). The XRD analysis carried out for this melt confirms the introduction of the modifier components into the AlSi7Mg alloy (Figure 4). In the radiograph, apart from the typical silumin components,

which are Al and Si, the presence of titanium, boron, and phosphorus compounds was found, which clearly confirms the transfer of the modifier to the treated alloy. It is obvious that the magnitude of the observed peaks for the modifier phases is not large. This is due to the fact that a small amount of individual chemical elements is introduced in relation to the weight of the treated alloy. After the modification of the master alloy AlTi0.25B0.05P0.1, further fragmentation of the lamellar α+β eutectic was found. A greater number of plates than in the previous case have parallel axes of symmetry, which proves another increase in the stability of eutectic growth and thus the stabilization of its crystallization process. The dendrites of the α phase are smaller in comparison to the previous modifier but still have large dimensions (Figure 2d). Changes in the microstructure result in mechanical properties, i.e., Rm = 178 Mpa, A = 5.3%, and H = 63 HB. These are the highest values for a master alloy containing 0.1% phosphorus (Figure 3). After modifying the silumin AlSi7Mg with the master alloy AlTi0.35B0.07P0.1, a slight degradation of the microstructure was found in relation to AlTi0.25B0.05P0.1. However, the eutectic plates still maintained equiaxiality. The dimensions of the primary α phase dendrites decreased (Figure 2e). The mechanical properties decreased within the measurement error to Rm = 175 Mpa, A = 4.9%, and H = 62 HB (Figure 3). Taking into account the number of tests carried out, it can be concluded that despite a slight decrease in mechanical properties, the tendency towards their decrease is correctly presented. After modification of the silumin master alloy AlTi0.45B0.09P0.1, an increase in the thickness of the eutectic β phase plates was noted, resulting in an increase in the thickness of the eutectic phases and a decrease in the size of the α phase dendrites (Figure 2f). As a result, the mechanical properties are further reduced to Re = 171 Mpa, A = 4.5%, and H = 61 HB (Figure 3). Comparing the changes in the microstructure of the AlSi7Mg silumin after modification with all master alloys, fragmentation of the primary α-phase dendrites was noted with an increase in the share of titanium and boron in the modifier. With the content of 0.1% phosphorus, the highest mechanical properties were obtained for the modifier AlTi0.25B0.05P0.1, containing 0.25% titanium and 0.05% boron.

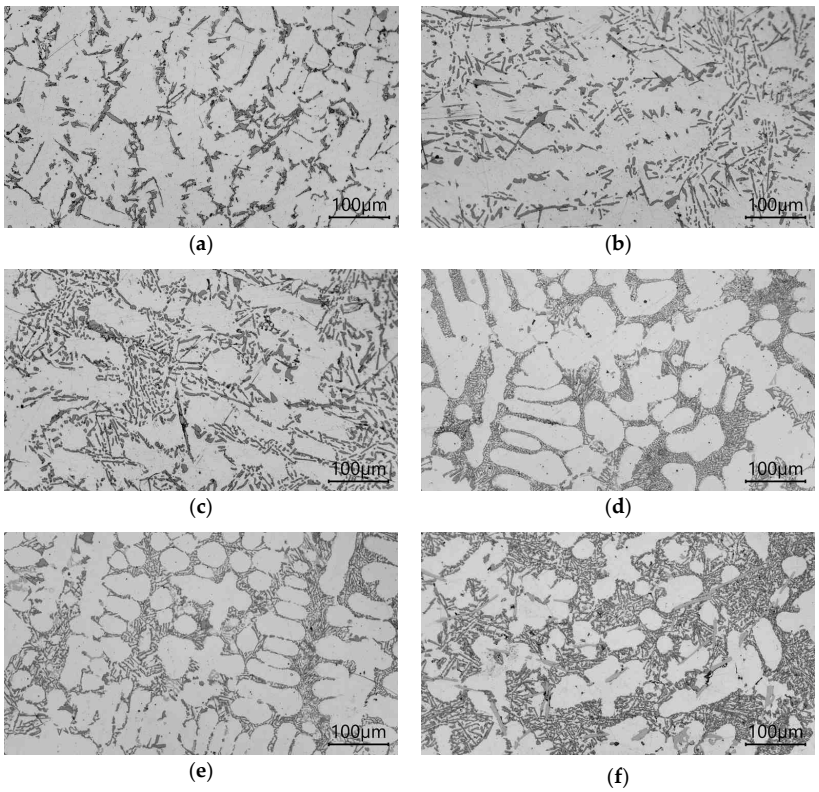

Figure 2. Microstructure the AlSi7Mg alloy without modification (**a**) and after modification with: (**b**) AlTi0.05B0.01P0.1, (**c**) AlTi0.15B0.03P0.1, (**d**) AlTi0.25B0.05P0.1, (**e**) AlTi0.35B0.07P0.1, (**f**) AlTi0.45B0.09P0.1.

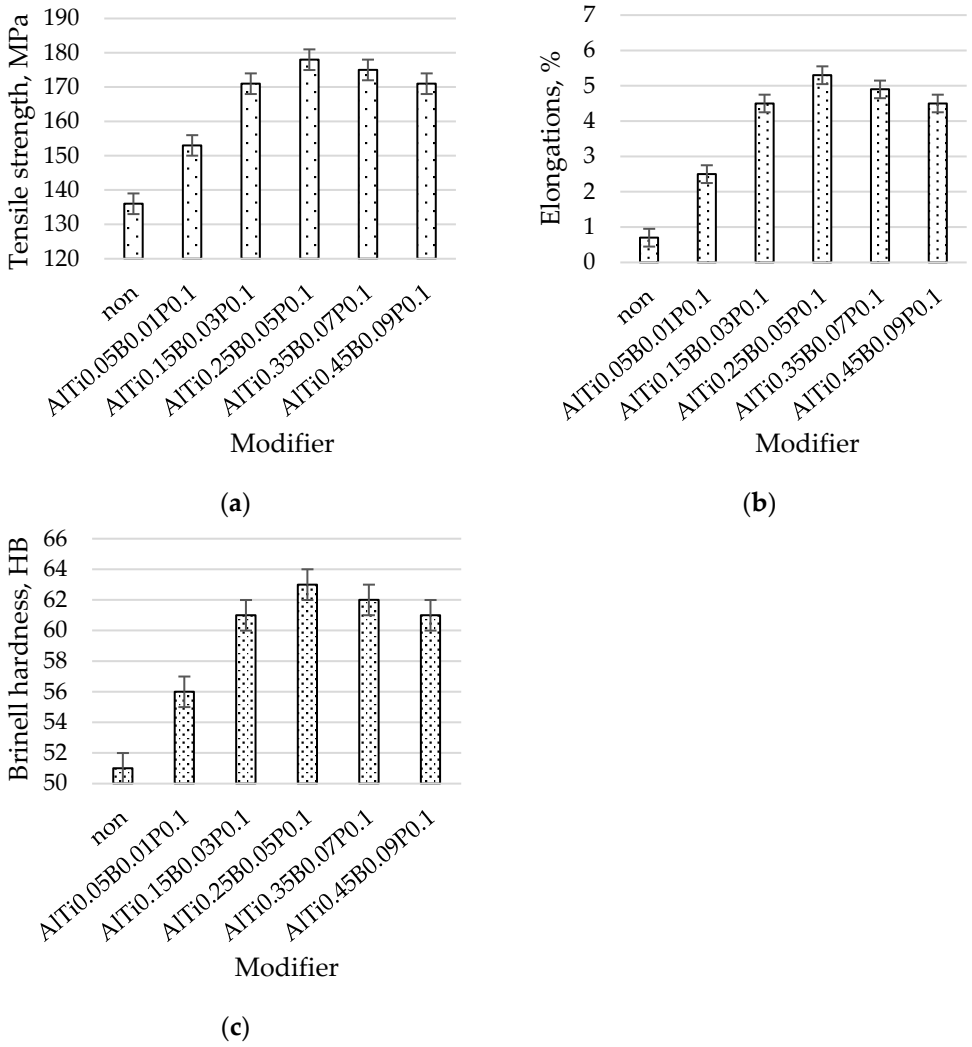

Figure 3. Mechanical properties the AlSi7Mg alloy without modification and after modification with AlTi0.05B0.01P0.1, AlTi0.15B0.03P0.1, AlTi0.25B0.05P0.1, AlTi0.35B0.07P0.1, AlTi0.45B0.09P0.1: (**a**) tensile strength, (**b**) elongations, (**c**) Brinell hardness.

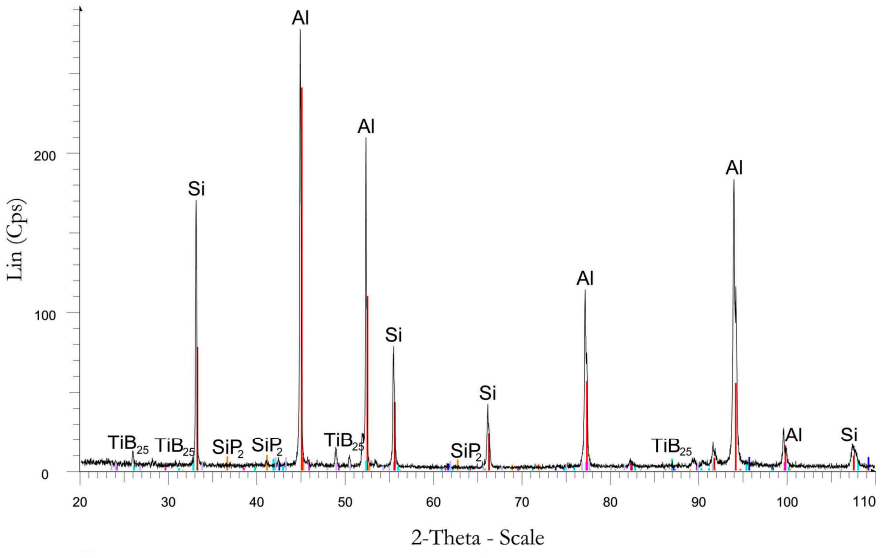

Figure 4. XRD of AlSi7Mg alloy with AlTi0.15B0.03P0.1.

After modification of the AlSi7Mg silumin with AlTi0.05B0.01P0.2, thus containing 0.05% Ti, 0.01% boron, and 0.2% phosphorus, calculated on the weight of the modified alloy, the microstructure already had parallel axes of the plates of the eutectic β phase. Thick precipitates of the β phase were still visible, indicating the final stage of transition as a result of modification into regular plates. The α phase had a dendritic structure. Based on the analysis of the overall microstructure, it was noted that the modification process with this master alloy proceeded in conditions close to stable, as evidenced by uniform axes distribution and similar thickness of the eutectic β phase with stabilized dimensions of the primary dendritic α phase (Figure 5a). The described microstructure is reflected in the mechanical properties: Rm = 169 MPa (Figure 6a), A = 4.3% (Figure 6b), and H = 61 HB (Figure 6c). After the modification of the silumin master alloy AlTi0.15B0.03P0.2, a much greater fragmentation of the microstructure was found than after the previously introduced modifier. In the eutectic β phase, it was difficult to find distinct plates with even axes of symmetry. The eutectic consisted of short twisted flakes, which is evidence of the thermodynamic system going beyond the stable growth range (Figure 5b). The primary β phase also gained finer dendrites than after AlTi0.05B0.01P0.2 modification (Figure 5a). The beneficial change in the microstructure resulted in an increase in the mechanical properties to the values of Rm = 177 MPa, A = 5.2%, and H = 63 HB (Figure 6). After introducing AlTi0.25B0.05P0.2 to the silumin in the form of a master alloy, a comparable eutectic shape was obtained as after AlTi0.15B0.03P0.2 modification but with a clearly finer eutectic α+β phase (Figure 5c). The primary dendritic α phase remained of similar size. The eutectic fragmentation of the alloy resulted in an increase in the mechanical properties to Rm = 186 MPa, A = 6.1%, and H = 65 HB (Figure 6). These were the highest mechanical properties for the master alloy series, containing 0.2% phosphorus. After the modification of the master alloy containing more titanium and boron (AlTi0.35B0.07P0.2), a similar shape of the α+β eutectic was observed, but a slight increase in the plate thickness of both its phases. A significant increase in the fragmentation of the primary α phase was also noted (Figure 5d). Such a microstructure has slightly lower mechanical properties than those discussed previously: Rm = 183 MPa, A = 5.7%, and H = 64 HB (Figure 6). After modification of the hypoeutectic silumin master alloy AlTi0.45B0.09P0.2, the microstructure gained a similar eutectic shape; unfortunately, another increase in the thickness of its components was noted (Figure 5e). There was no change in the size of the primary α phase dendrites. A slight degradation in the microstructure resulted in a further reduction in the analyzed mechanical properties to Ra = 178 MPa, A = 5.3%, and H = 63 HB (Figure 6). The changes in hardness for individual test points did not seem to be large, but it should be emphasized that the stability of hardness measurements was 100% for some samples, so the measurement error was 0 HB. Analyzing the average hardness measurement error for all points of the discussed test plan for 0.2% of phosphorus, the average error was found at the level of 0.23 HB.

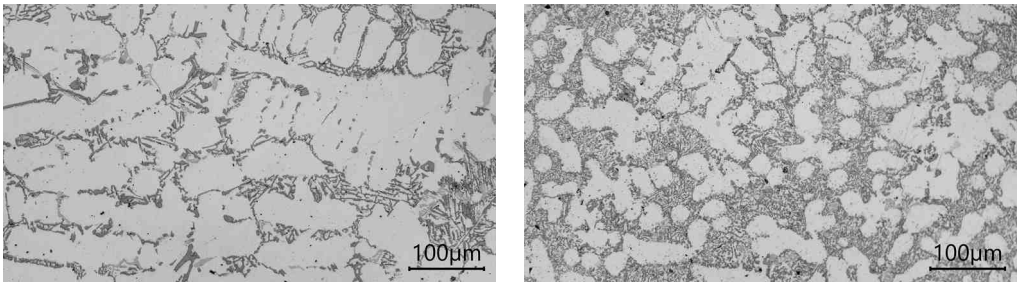

(**a**) (**b**)

Figure 5. *Cont.*

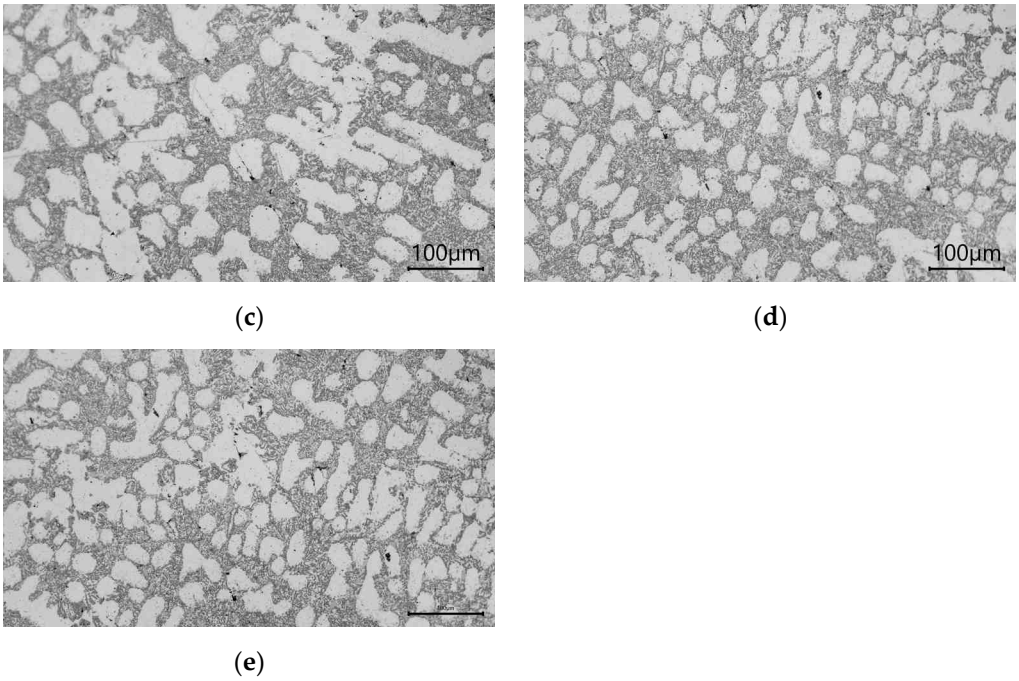

Figure 5. Microstructure the AlSi7Mg alloy with: (**a**) AlTi0.05B0.01P0.2, (**b**) AlTi0.15B0.03P0.2, (**c**) AlTi0.25B0.05P0.2, (**d**) AlTi0.35B0.07P0.2, (**e**) AlTi0.45B0.09P0.2.

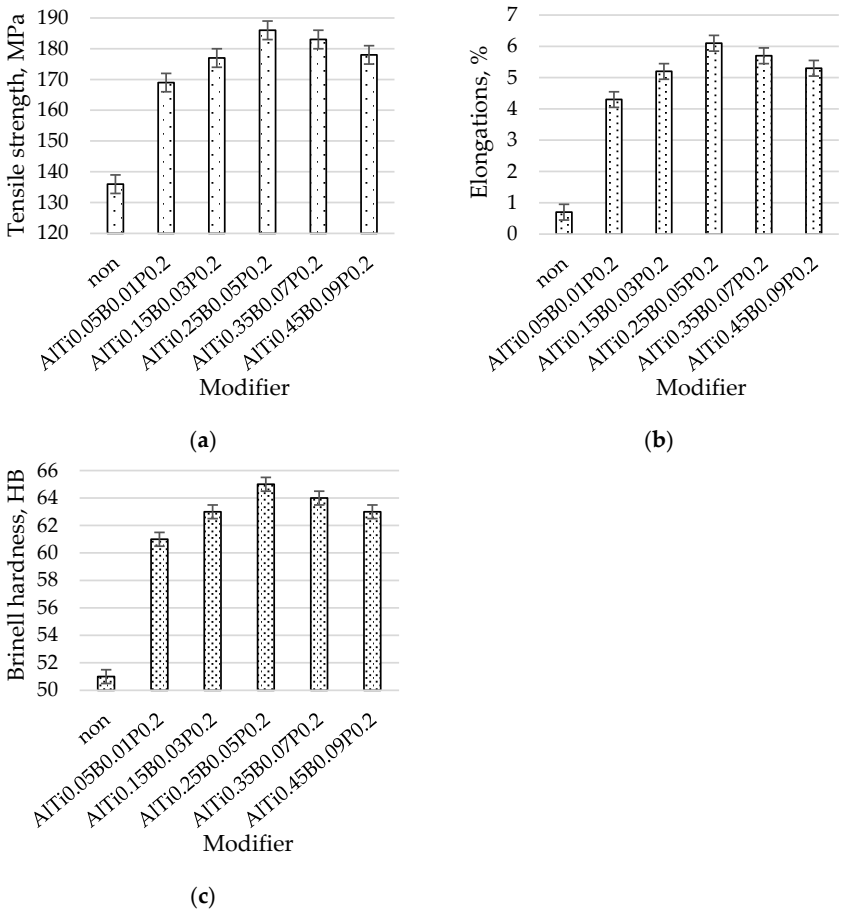

Figure 6. Mechanical properties the AlSi7Mg alloy without modification and after modification with AlTi0.05B0.01P0.2, AlTi0.15B0.03P0.2, AlTi0.25B0.05P0.2, AlTi0.35B0.07P0.2, AlTi0.45B0.09P0.2: (**a**) tensile strength, (**b**) elongations, (**c**) Brinell hardness.

In the third stage of the research, a master alloy with analogous compositions as in the first two stages was used, but with a phosphorus content of 0.3% in relation to the weight of the treated silumin AlSi7Mg. After modification of the silumin AlTi0.05B0.01P0.3 master alloy, thick plates of the eutectic β phase were obtained against the background of the disordered primary α phase. Partial systematization of the eutectic β phase was visible in the microstructure, which indicated the beginning of stabilization of the eutectic crystallization process. In the α phase, it was difficult to find the dendritic system (Figure 7a). The obtained microstructure determined the relatively low mechanical properties of the alloy Rm = 160 MPa (Figure 8a), A = 3.3% (Figure 8b), and H = 56 HB (Figure 8c). After modifying the silumin AlTi0.15B0.03P0.3 master alloy, a change in the shape of the eutectic α+β phases was observed. The β phase had changed and lost the shape of long thick plates. The distribution of the eutectic phases became irregular, which proves the lack of crystallization stability. A modified microstructure of the α+β eutectic was obtained. Large dendrite arms could be seen in the α phase (Figure 7b). Modification of the eutectic and the α phase resulted in an increase in the tested mechanical properties (Figure 8). Rm = 175MPa, A = 5.0%, and H = 62HB were obtained. After modification of the AlTi0.25B0.05P0.3 master alloy, a fine eutectic composed of α and β phases was obtained. The character of eutectic resembled its geometric form described previously. The presence of the primary α phase in the form of clearly visible dendrites (Figure 7c) with smaller dimensions than after the AlTi0.15B0.03P0.3 modification, i.e., lower content of titanium and boron, was observed. The effect of obtaining a finer eutectic and the α phase with smaller dimensions was to achieve higher mechanical properties. Tensile strength Rm = 181 MPa, elongation A = 5.5%, and hardness H = 63 HB (Figure 8). The values of mechanical strength at this test point were the highest for the analyzed third series, in which the share of phosphorus was set at 0.3% of the weight of the treated silumin. After introducing AlTi0.35B0.07P0.3 into the silumin, a primary α phase of comparable size was obtained. The α+β eutectic consisted of fine plates of the β phase. The geometric shape of the β phase was diverse. The presence of most of the β phase in an irregular form was noted as well as the presence of fine plates with a parallel arrangement of symmetry axes. This arrangement of the eutectic indicated the occurrence of two processes during crystallization, and then the growth of stable and unstable eutectic (Figure 7d). The equivalent of the microstructure are the mechanical properties of silumin with the following parameters: Rm = 177 MPa, A = 5.3%, and H = 62 HB (Figure 8). Therefore, a slight decrease in strength properties was noted in relation to the properties of the tested silumin after AlTi0.25B0.05P0.3 modification. This may indicate that increasing the content of titanium and boron at a constant 0.3% phosphorus content from 0.25 and 0.05 to 0.35 and 0.07%, respectively, in relation to the weight of the treated alloy causes a slight degradation of the microstructure and a slight decrease in the analyzed mechanical properties of AlSi7Mg alloy. After the modification of the silumin AlTi0.45B0.09P0.3, a slight increase in the thickness of the eutectic β phase plates and a slight fragmentation of the α phase with a dendritic system were noted. Similarly to the modification of the AlTi0.35B0.07P0.3 master alloy, there were two areas in the eutectic proper for different crystallization courses of the silumin eutectic. In the areas of occurrence of β phase plates with parallel arrangements of their axes of symmetry, their elongation was observed. This is a sign of degradation of the microstructure (Figure 7e). The changes in the microstructure are reflected in the reduction in the mechanical properties in relation to the parameters of the alloy described after the AlTi0.35B0.07P0.3 modification. The mechanical properties of the analyzed test point are as follows: Rm = 174 MPa, A = 4.9%, and H = 62 HB. Thus, the reduction in the tested mechanical parameters was not large, but it confirms their tendency to decrease with the increase in the amount of titanium and boron introduced.

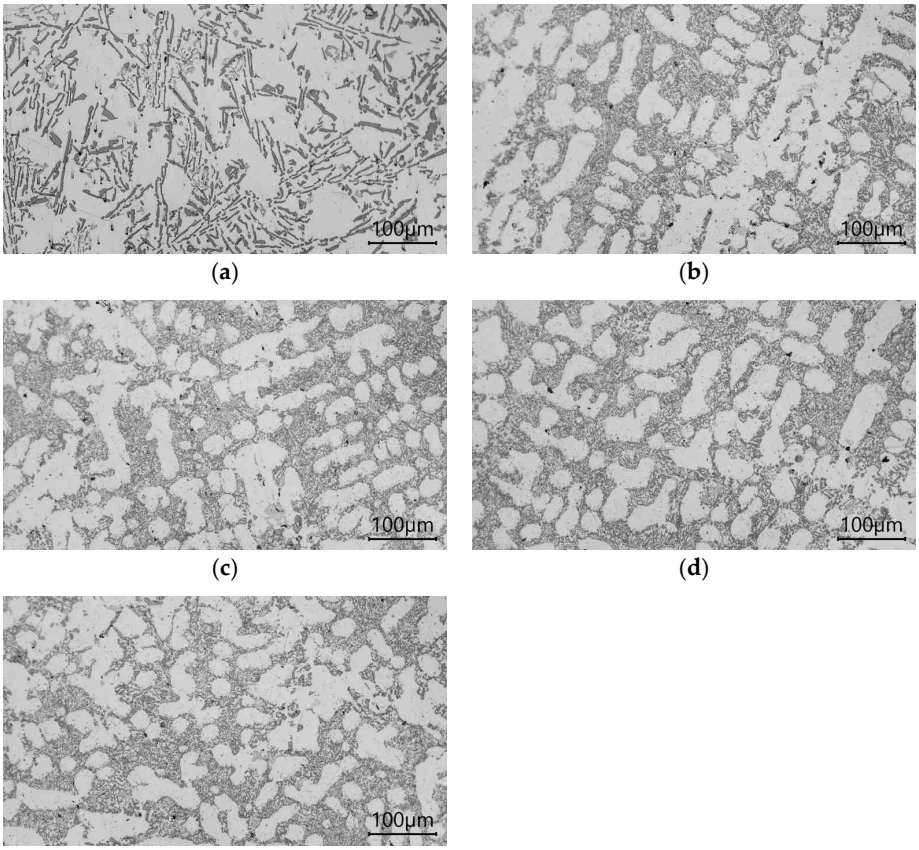

Figure 7. Microstructure the AlSi7Mg alloy with: (**a**) AlTi0.05B0.01P0.3, (**b**) AlTi0.15B0.03P0.3, (**c**) AlTi0.25B0.05P0.3, (**d**) AlTi0.35B0.07P0.3, (**e**) AlTi0.45B0.09P0.3.

The results of the tests showed that the introduction of phosphorus to the master alloy affects the strength properties of the hypoeutectic silumin. For all three analyzed series of tests in which phosphorus was introduced into the master alloy at a constant level (0.1, 0.2, and 0.3% in relation to the mass of modified silumin), it was shown that the nature of changes in the analyzed mechanical properties depends mainly on the content of titanium and boron (Figures 3, 5 and 7). However, the share of phosphorus in the master alloy in combination with the presence of titanium and boron affects the level of mechanical properties obtained. This is confirmed by the results of earlier studies in which the authors found that the eutectic Al-Si alloy modified with Al-3P had an increase in tensile strength and elongation. The highest mechanical properties were obtained for 0.4 wt. Al-3P [79].

The highest properties were obtained for 0.2% phosphorus in relation to the mass of modified silumin. For each of the three series of tests, the highest strength properties (in relation to the results obtained in each series of tests) were obtained for the master alloy with the composition AlTi0.25B0.05Px, regardless of the phosphorus content. The increase in the share of titanium and boron did not increase the mechanical properties of the analyzed alloy but even slightly decreased them. Thus, 0.25% Ti and 0.05% B, as well as the content of 0.2%, were considered the optimal components for the tests carried out. In the studies conducted on the Al7%Si alloy [58], the authors noted that at a concentration of 2 to 3 ppm of phosphorus, solidification took place mainly in the interdendritic spaces of the α phase on AlP particles serving as heterogeneous nuclei for the eutectic β phase rich in silicon. An increase in the nucleation rate of the eutectic phase was also observed with an increase in the phosphorus content by at least one order of magnitude. The work [80] presents the results confirming a clear and direct lattice relationship between the centrally located AlP particles and the silicon surrounding them in the hypoeutectic Al-Si alloy, which confirms the modifying capabilities of phosphorus with respect to the α+β eutectic.

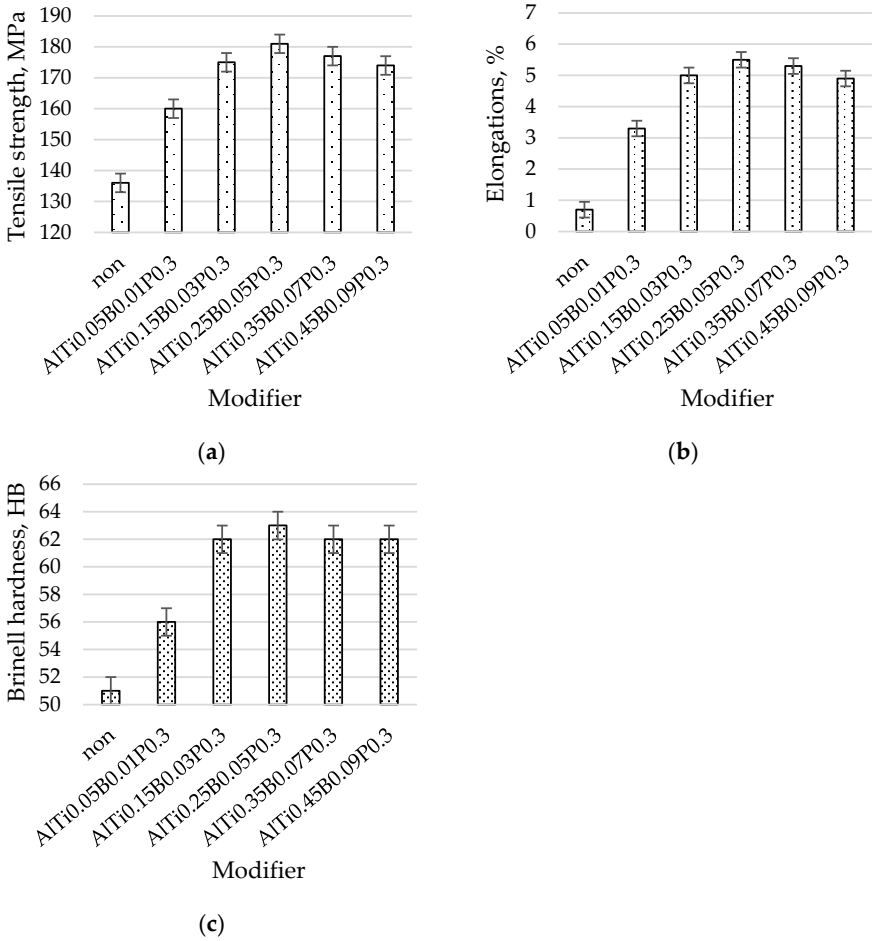

Figure 8. Mechanical properties the AlSi7Mg alloy without modification and after modification with AlTi0.05B0.01P0.3, AlTi0.15B0.03P0.3, AlTi0.25B0.05P0.3, AlTi0.35B0.07P0.3, AlTi0.45B0.09P0.3: (**a**) tensile strength, (**b**) elongations, (**c**) Brinell hardness.

Analyzing the size of the primary α phase and the eutectic morphology, it was found that the eutectic morphology had a much stronger influence on the mechanical properties of silumin than the soft and plastic size of the α phase. This confirms the observed regularity that with fragmentation of the α phase and slight degradation of the α+β eutectic, the mechanical properties decrease. The addition of AlTi5B1 has been widely recognized to disintegrate the microstructure of hypoeutectic silumins [1,73,75,76]. At the same time, many researchers usually point to the effectiveness of titanium alone, as well as when combined with boron. The obtained results only confirm the previous observations on titanium and boron without analyzing the effectiveness of each of them (they were used in a constant proportion). In the analyzed range of the addition of titanium and boron, together with the increase in their content, fragmentation of the silumin microstructure, mainly the primary dendrites of the α phase, was noted.

4. Conclusions

Based on the results of the research, it was found that:

- By changing the content of titanium and boron (5:1 ratio) in the aluminum-based master alloy in the presence of phosphorus, it is possible to control the microstructure and mechanical properties of hypoeutectic silumin;
- Phosphorus in the master alloy, based on aluminum, titanium, and boron, affects the microstructure and mechanical properties of hypoeutectic silumin AlSi7Mg;
- It was shown that with the ratio of titanium to boron in the aluminum-based master alloy in the presence of phosphorus, the highest mechanical properties were achieved

for the AlTi0.25B0.05P0.2 master alloy with the content of 0.25% titanium, 0.05% boron, and 0.2% phosphorus in relation to the weight of the modified hypoeutectic silumin.

Funding: This research received no external funding.

Data Availability Statement: Not applicable.

Conflicts of Interest: The author declares no conflict of interest.

References

1. Michna, S.; Lukac, I.; Ocenasek, V.; Koreny, R.; Drapala, J.; Schneider, H.; Miskufova, A. *Encyclopaedia of Aluminium*; Adin s.r.o. Presov: Prešov, Slovakia, 2005. (In Czech)
2. Selejdak, J.; Ulewicz, R.; Ingaldi, M. The evaluation of the use of a device for producing metal elements applied in civil engineering. In Proceedings of the 23rd International Conference on Metallurgy and Materials, Brno, Czech Republic, 21–23 May 2014; pp. 1882–1888.
3. Koreček, D.; Solfronk, P.; Sobotka, J. Research of Mechanical Properties of the Aluminium Alloy Amag 6000 under the Plane Stress State Conditions. *Manuf. Technol.* **2022**, *22*, 709–712. [CrossRef]
4. Dash, S.S.; Chen, D. A Review on Processing—Microstructure–Property Relationships of Al-Si Alloys: Recent Advances in Deformation Behavior. *Metals* **2023**, *13*, 609. [CrossRef]
5. Šurdová, Z.; Kuchariková, L.; Tillová, E.; Pastierovičová, L.; Chalupová, M.; Uhríčik, M.; Mikolajčík, M. The Influence of Fe Content on Corrosion Resistance of secondary AlSi7Mg0.3 Cast Alloy with Increased Fe-content. *Manuf. Technol.* **2022**, *22*, 598–604. [CrossRef]
6. Heidarzadeh, A.; Khorshidi, M.; Mohammadzadeh, R.; Khajeh, R.; Mofarrehi, M.; Javidani, M.; Chen, X.-G. Multipass Friction Stir Processing of Laser-Powder Bed Fusion AlSi10Mg: Microstructure and Mechanical Properties. *Materials* **2023**, *16*, 1559. [CrossRef]
7. Józwik, J.; Ruggiero, A.; Leleń, M. Microscopic Analysis of the Surface Morphology of Multilayer Structures of the Aluminum Alloy—Silicon Type after Water Jet Cutting. *Manuf. Technol.* **2022**, *22*, 693–702.
8. Kurz, W.; Fisher, D.J. *Fundamentals of Solidifications*; TTP: Trasadingen, Switzerland, 1986.
9. Flemings, M.C. Solidification Processing. *Metall. Mater. Tran.* **1974**, *5*, 2121–2134. [CrossRef]
10. Tenkamp, J.; Stern, F.; Walther, F. Uniform Fatigue Damage Tolerance Assessment for Additively Manufactured and Cast Al-Si Alloys: An Elastic-Plastic Fracture Mechanical Approach. *Addit. Manuf. Lett.* **2022**, *3*, 100054. [CrossRef]
11. Magnin, P.; Mason, J.T.; Trivedi, R. Growth of irregular eutectics and the Al-Si system. *Acta Metall. Et Mater.* **1991**, *39*, 469–480. [CrossRef]
12. Novak, M.; Naprstkova, N.; Ruzicka, L. New ways in aluminium alloys grinding. *Key Eng. Mater.* **2012**, *496*, 132–137. [CrossRef]
13. Khalaf, A.A. Microstructure evolution of Al-Si hypoeutectic alloys prepared by controlled diffusion solidification. *Int. J. Adv. Manuf. Technol.* **2022**, *120*, 5003–5014. [CrossRef]
14. Michna, Š.; Hren, I.; Cais, J.; Michnová, L. The research of the different properties and production parameters having influence on deep-drawing sheets made of $AlMg_3$ alloy. *Manuf. Technol.* **2020**, *20*, 347–354. [CrossRef]
15. Fang, L.; Fuxiao, Y.; Dazhi, Z.; Liang, Z. Microstructure and mechanical properties of an Al–12.7Si–0.7Mg alloy processed by extrusion and heat treatment. *Mater. Sci. Eng.* **2011**, *528*, 3786–3790.
16. Dahle, A.K.; Nogita, K.; Mcdonald, S.D.; Dinnis, C.; Lu, L. Eutectic modification and microstructure development in Al–Si Alloys. *Mater. Sci. Eng.* **2005**, *413–414*, 243–248. [CrossRef]
17. Martinovsky, M.; Madl, J. The effect of different modifiers on cutting temperature in turning of AlSi7Mg0.3 alloy. *Manuf. Technol.* **2018**, *18*, 950–953. [CrossRef]
18. Zhang, Z.W.; Wang, J.L.; Zhang, Q.L.; Zhang, S.P.; Shi, Q.N.; Qi, H.R. Research on Grain Refinement Mechanism of 6061 Aluminum. Alloy Processed by Combined SPD Methods of ECAP and MAC. *Materials* **2018**, *11*, 1246. [CrossRef]
19. Naprstkova, N.; Kraus, P.; Stancekova, D. Calcium and its using for modification of AlSi7Mg0.3 alloy from view of final microstructure and hardness. *Proc. Eng. Rural. Dev.* **2018**, *17*, 2003–2008.
20. Lipiński, T.; Szabracki, P. Mechanical Properties of AlSi9Mg Alloy with a Sodium Modifier. *Solid State Phenom.* **2015**, *223*, 78–86. [CrossRef]
21. Nova, I.; Frana, K.; Sobotka, I.; Solfronk, P.; Korecek, D.; Novakova, I. Production of porous aluminium using sodium chloride. *Manuf. Technol.* **2019**, *19*, 817–822. [CrossRef]
22. Nová, I.; Fraňa, K.; Lipiński, T. Monitoring of the interaction of aluminum alloy and sodium chloride as the basis for ecological production of expanded aluminum. *Phys. Met. Metallogr.* **2021**, *122*, 1288–1300. [CrossRef]
23. Lipinski, T.; Szabracki, P. Modification of the hypo-eutectic Al-Si alloys with an exothermic modifier. *Arch. Metall. Mater.* **2013**, *58*, 453–458. [CrossRef]
24. Lipiński, T. Use Properties of the AlSi9Mg Alloy with Exothermical Modifier. *Manuf. Technol.* **2011**, *11*, 44–49.
25. El Sebaie, O.; Samuel, A.M.; Samuel, F.H.; Doty, H.W. The effects of mischmetal, cooling rate and heat treatment on the eutectic Si particle characteristics of A319.1, A356.2 and A413.1 Al–Si casting alloys. *Mater. Sci. Eng.* **2008**, *480*, 342–355. [CrossRef]
26. Liao, H.; Sun, Y.; Sun, G. Effect of Al-5Ti-1B on the microstructure of near-eutectic Al-13.0%Si alloys modified with Sr. *J. Mater. Sci.* **2002**, *37*, 3489–3495. [CrossRef]

27. Hren, I.; Svobodova, J. Fractographic analysis of strontium-modified Al-Si alloys. *Manuf. Technol.* **2018**, *18*, 900–905. [CrossRef]
28. Lei, W.B.; Liu, X.T.; Wang, W.M.; Sun, Q.; Xu, Y.Z.; Cui, J.Z. On the influences of Li on the microstructure and properties of hypoeutectic Al-7Si alloy. *J. Alloys Compd.* **2017**, *729*, 703–709. [CrossRef]
29. Konovalov, S.V.; Zagulyaev, D.V.; Ivanov, Y.F.; Gromov, V.E. Effect of yttrium oxide modification of Al-Si alloy on microhardness and microstructure of surface layers. *Metalurgija* **2018**, *57*, 253–256.
30. Zupanič, F.; Žist, S.; Albu, M.; Letofsky-Papst, I.; Burja, J.; Vončina, M.; Bončina, T. Dispersoids in Al-Mg-Si Alloy AA 6086 Modified by Sc and Y. *Materials* **2023**, *16*, 2949. [CrossRef]
31. Xiufang, B.; Weimin, W.; Jingyu, Q. Liquid structure of Al-12.5% Si alloy modified by antimony. *Mater. Charact.* **2001**, *46*, 25–29. [CrossRef]
32. Wang, Q.; Kang, N.; Mansori, M.; Yu, T.; Hadrouz, M.; Huang, X.; Lin, X. Effect of Ti on the microstructure and wear behavior of a selective laser melted Al-Cu-Mg-Si alloy. *Wear* **2023**, *523*, 204790. [CrossRef]
33. Wu, Y.N.; Zhang, J.F.; Liao, H.C.; Li, G.Y.; Wu, Y.P. Development of high performance near eutectic Al-Si-Mg alloy profile by micro alloying with Ti. *J. Alloys Compd.* **2016**, *660*, 141–147. [CrossRef]
34. Zhang, S.; Yi, W.; Zhong, J.; Gao, J.; Lu, Z.; Zhang, L. Computer Alloy Design of Ti Modified Al-Si-Mg-Sr Casting Alloys for Achieving Simultaneous Enhancement in Strength and Ductility. *Materials* **2023**, *16*, 306. [CrossRef] [PubMed]
35. Yuying, W.; Xiangfa, L.; Xiufang, B. Effect of boron on the microstructure of near-eutectic Al–Si alloys. *Mater. Charact.* **2007**, *58*, 205–209. [CrossRef]
36. Lipiński, T. Modification of Al-Si alloys with the use of a homogenous modifiers. *Arch. Metall. Mater.* **2008**, *53*, 193–197.
37. Zhang, X.; Yan, L.; Li, Z.; Li, X.; Gao, G.; Yan, H.; Wen, K.; Zhang, Y.; Xiong, B. Effects of Cu Addition on Age Hardening Behavior and Mechanical Properties of High-Strength Al-1.2Mg-1.2Si Alloy. *Materials* **2023**, *16*, 3126. [CrossRef] [PubMed]
38. Cui, J.; Chen, J.; Li, Y.; Luo, T. Enhancing the Strength and Toughness of A356.2-0.15Fe Aluminum Alloy by Trace Mn and Mg Co-Addition. *Metals* **2023**, *13*, 1451. [CrossRef]
39. Wang, H.; He, L.; Zhang, Q.; Yuan, Y. Influence of Ni Contents on Microstructure and Mechanical Performance of AlSi10Mg Alloy by Selective Laser Melting. *Materials* **2023**, *16*, 4679. [CrossRef]
40. Ourdjini, A.; Yilmaz, F.; Hamed, Q.S.; Elliott, R. Microstructure and mechanical properties of directionally solidified Al-Si eutectic alloys with and without antimony. *Mater. Sci. Technol.* **1992**, *8*, 764–776. [CrossRef]
41. Pierantoni, M.; Gremaud, M.; Magnin, P.; Stoll, D.; Kurz, W. The coupled zone of rapidly solidified Al-Si alloys in laser treatment. *Acta Metall. Et Mater.* **1992**, *40*, 1637–1644. [CrossRef]
42. Li, S.M.; Quan, Q.R.; .Li, X.; Fu, H.Z. Increasing the growth velocity of coupled eutectics in directional solidification of off-eutectic alloys. *J. Cryst. Growth* **2011**, *314*, 279–284. [CrossRef]
43. Wołczyński, W.; Cupryś, R.; Major, B. Averge intrelanellar spacing in oriented eutectic growth of irregular structure. *Arch. Metall.* **1998**, *43*, 309–320.
44. Yang, J.; Oliveira, J.P.; Li, Y.; Tan, C.; Gao, C.; Zhao, Y.; Yu, Z. Laser techniques for dissimilar joining of aluminum alloys to steels: A critical review. *J. Mater. Process. Technol.* **2022**, *301*, 117443. [CrossRef]
45. Zaguliaev, D.; Konovalov, S.; Ivanov, Y.; Gromov, V. Effect of electron-plasma alloying on structure and mechanical properties of Al-Si alloy. *Appl. Surf. Sci.* **2019**, *498*, 143767. [CrossRef]
46. Lipinski, T. Effect of combinative cooled addition of strontium and aluminium on mechanical properties AlSi12 alloy. *J. Achiev. Mater. Manuf. Eng.* **2017**, *83*, 5–11. [CrossRef]
47. Pastircák, R.; Bruna, M.; Matejka, M.; Bolibruchová, D. Effect of Input Parameters on the Structure and Properties of Castings Obtained via Crystallization under Pressure. *Metals* **2023**, *13*, 1424. [CrossRef]
48. Liu, Y.; Chen, T. Effect of Standing Time after Mixing on the Mixture Microstructure of an Al-Si Alloy during Controlled Diffusion Solidification with Simultaneous Mixing. *Metals* **2023**, *13*, 733. [CrossRef]
49. Wang, X.; Liu, Y.; Huang, Y. Improving Precipitation in Cryogenic Rolling 6016 Aluminum Alloys during Aging Treatment. *Materials* **2023**, *16*, 3336. [CrossRef]
50. Di Egidio, G.; Martini, C.; Börjesson, J.; Ghassemali, E.; Ceschini, L.; Morri, A. Influence of Microstructure on Fracture Mechanisms of the Heat-Treated AlSi10Mg Alloy Produced by Laser-Based Powder Bed Fusion. *Materials* **2023**, *16*, 2006. [CrossRef]
51. Lipiński, T.; Bramowicz, M.; Szabracki, P. The Microstructure and Mechanical Properties of Al-7%SiMg Alloy Treated with an Exothermic Modifier Containing Na and B. *Solid State Phenom.* **2013**, *203–204*, 250–253. [CrossRef]
52. Gebril, M.A.; Omar, M.Z.; Mohamed, I.F.; Othman, N.K.; Irfan, O.M. Microstructure Refinement by a Combination of Heat Treatment and Thixoforming Process Followed by Severe Plastic Deformation and Their Effects on Al-Si Alloy Hardness. *Metals* **2022**, *12*, 1972. [CrossRef]
53. Nogita, K.; Knuutinen, A.; McDonald, S.D.; Dahle, A.K. Mechanisms of eutectic solidification in Al–Si alloys modified with Ba, Ca, Y and Yb. *J. Light Met.* **2001**, *1*, 219–228. [CrossRef]
54. Lipiński, T. Effect of Modifier Form on Mechanical Properties of Hypoeutectic Silumin. *Materials* **2023**, *16*, 5250. [CrossRef] [PubMed]
55. Knuutinen, A.; Nogita, K.; McDonald, S.D.; Dahle, A.K. Modification of Al–Si alloys with Ba, Ca, Y and Yb. *J. Light Met.* **2001**, *1*, 229–240. [CrossRef]
56. Tang, T.; Lai, H.; Sheng, Z.; Gan, C.; Xing, P.; Luo, X. Effect of tin addition on the distribution of phosphorus and metallic impurities in Si–Al alloys. *J. Cryst. Growth* **2016**, *453*, 13–19. [CrossRef]

57. Lipiński, T. Modification of Al-11% Si Alloy with Cl—Based Modifier. *Manuf. Technol.* **2015**, *15*, 581–587. [CrossRef]
58. Ludwig, T.H.; Schaffer, P.L.; Arnberg, L. Influence of phosphorus on the nucleation of eutectic silicon in Al–Si alloys. *Metall. Mater. Trans.* **2013**, *44*, 5796–5805. [CrossRef]
59. Wang, T.; Fu, H.; Chen, Z.; Xu, J.; Zhu, J.; Cao, F.; Li, T. A novel fading-resistant Al–3Ti–3B grain refiner for Al–Si alloys. *J. Alloys Compd.* **2012**, *511*, 45–49. [CrossRef]
60. Grobner, J.; Mirkovic, D.; Schmid-Fetzer, R. Thermodynamic aspects of grain refinement of Al–Si alloys using Ti and B. *Mater. Sci. Eng.* **2005**, *395*, 10–21. [CrossRef]
61. Lipiński, T. Effect of Sr, Ti and B additions as powder and a preliminary alloy with Al on microstructure and tensile strength AlSi9Mg alloy. *Manuf. Technol.* **2019**, *19*, 807–812. [CrossRef]
62. Li, J.G.; Zhang, B.Q.; Wang, L.; Yang, W.Y.; Ma, H.T. Combined effect and its mechanism of Al-3wt.%Ti-4wt.%B and Al-10wt.%Sr master alloy on microstructures of Al-Si-Cu alloy. *Mater. Sci. Eng.* **2002**, *328*, 169–176. [CrossRef]
63. Lipiński, T. Double modification of AlSi9Mg alloy with boron, titanium and strontium. *Arch. Metall. Mater.* **2015**, *60*, 2415–2419. [CrossRef]
64. Xua, J.; Li, Y.; Maa, K.; Fub, Y.; Guoc, E.; Chenc, Z.; Gud, Q.; Hane, Y.; Wangc, T.; Li, Q. In-situ observation of grain refinement dynamics of hypoeutectic Al-Si alloy inoculated by Al-Ti-Nb-B alloy. *Scr. Mater.* **2020**, *187*, 142–147. [CrossRef]
65. Kakhidze, N.; Valikhov, V.; Selikhovkin, M.; Khrustalyov, A.; Zhukov, I.; Vasiliev, S.; Vorozhtsov, A. Effects of ErF3 Particles on the Structure and Physicomechanical Properties of A359 Alloy. *Metals* **2023**, *13*, 1463. [CrossRef]
66. Lu, L.; Dahle, A.K. Effects of combined additions of Sr and AlTiB grain refiners in hypoeutectic Al–Si foundry alloys. *Mater. Sci. Eng.* **2006**, *435–436*, 288–296. [CrossRef]
67. Meng, C.; Su, C.; Liu, Z.; Liao, D.; Rong, X.; Li, Y.; Tang, H.; Wang, J. Synergistic Effect of RE (La, Er, Y, Ce) and Al-5Ti-B on the Microstructure and Mechanical Properties of 6111Aluminum Alloy. *Metals* **2023**, *13*, 606. [CrossRef]
68. Prasada Rao, A.K.; Das, K.; Murty, B.S.; Chakraborty, M. Al–Ti–C–Sr master alloy—A melt inoculant for simultaneous grain refinement and modification of hypoeutectic Al–Si alloys. *J. Alloys Compd.* **2009**, *480*, L49–L51.
69. Sofyan, B.T.; Kharistal, D.J.; Trijati, L.; Purba, K.; Susanto, R.E. Grain refinement of AA333 aluminium cast alloy by Al–Ti granulated flux. *Mater. Des.* **2010**, *31*, S36–S43. [CrossRef]
70. Nogita, K.; Dahle, A.K. Effects of boron on eutectic modification of hypoeutectic Al–Si alloys. *Scr. Mater.* **2003**, *48*, 307–313. [CrossRef]
71. Kori, S.A.; Murty, B.S.; Chakraborty, M. Development of an efficient grain refiner for Al–7Si alloy and its modification with strontium. *Mater. Sci. Eng.* **2000**, *283*, 94–104. [CrossRef]
72. Shu, D.; Sun, B.; Mi, J.; Grant, P.S. A quantitative study of solute diffusion field effects on heterogeneous nucleation and the grain size of alloys. *Acta Mater.* **2011**, *59*, 2135–2144. [CrossRef]
73. Górny, Z. *Foundry Alloys of Non-Ferrous Metals. Odlewnicze Stopy Metali Nieżelaznych*; WNT: Warsaw, Poland, 1992. (In Polish)
74. Murty, B.S.; Kori, S.A.; Venkateswarlu, K.; Bhat, R.R.; Chakraborty, M. Manufacture of Al–Ti–B master alloys by the reaction of complex halide salts with molten aluminium. *J. Mater. Process. Technol.* **1999**, *89–90*, 152–158. [CrossRef]
75. Romankiewicz, F. Research on the modification of the AlSi7Mg alloy with additions of AlTi5B1 and AlSr10. Badania nad modyfikacją stopu AlSi7Mg dodatkami AlTi5B1 i AlSr10. In Proceedings of the II Konferencja—Zjawiska Powierzchniowe w Procesach Odlewniczych, Poznań, Kołobrzeg; 1994; pp. 93–103. (In Polish).
76. Wen, Y.; Wu, Y.; Wu, Y.; Gao, T.; Wei, Z.; Liu, X. Effect of Al-5Ti-0.25C-0.25B and Al-5Ti-1B Master Alloys on the Microstructure and Mechanical Properties of Al-9.5Si-1.5Cu-0.8Mn-0.6Mg Alloy. *Materials* **2023**, *16*, 1246. [CrossRef] [PubMed]
77. *EN ISO 6892-1:2019*; Metallic Materials—Tensile Testing Part 1: Method of Test at Room Temperature. International Organization for Standardization: Geneva, Switzerland, 2019.
78. *ISO 6506-1:2014*; Metallic Materials—Brinell Hardness Test—Part 1: Test Method. International Organization for Standardization: Geneva, Switzerland, 2014.
79. Wang, S.; Fu, M.; Li, L.; Wang, J.; Su, X. Microstructure and mechanical properties of Al–Si eutectic alloy modified with Al–3P master alloy. *J. Mater. Process. Technol.* **2018**, *255*, 105–109. [CrossRef]
80. Nogita, K.; Mcdonald, S.D.; Tsujimoto, K.; Yasuda, K.; Dahle, A.K. Aluminium phosphide as a eutectic grain nucleus in hypoeutectic Al–Si alloys. *J. Electron. Microsc.* **2004**, *53*, 361–369. [CrossRef] [PubMed]